

Cardiovascular Translational Medicine (VIII)

Noninvasive Cardiovascular Imaging Techniques for Basic Science Research: Application to Cellular Therapeutics

Wesley D. Gilson^{a,b} and Dara L. Kraitchman^b^aImaging & Visualization, Siemens Corporate Research, Inc. Baltimore, Maryland, USA^bRussell H. Morgan Department of Radiology and Radiological Science, The Johns Hopkins University, Baltimore, Maryland, USA

Cell therapy continues to be an active area of basic science research with early promise in the treatment of cardiovascular diseases. However, there are many unknowns including the mechanisms by which they work, the most useful cell types, the most efficient delivery strategies, and their safety. Noninvasive imaging provides a wide array of tools to quantitatively address many of these unknowns. This article reviews echocardiography, magnetic resonance imaging, computed tomography, positron emission tomography and single photon emission tomography in the context of imaging cellular therapeutics to demonstrate how these modalities are being used to answer some of these questions.

Key words: *Stem cells. Magnetic resonance imaging. Echocardiography. Radionuclide imaging.*

Técnicas no invasivas de imagen cardiovascular en investigación básica: aplicación en la terapia celular

La terapia celular continúa siendo un área muy activa en el campo de la investigación básica, con resultados iniciales prometedores en el tratamiento de las enfermedades cardiovasculares. Sin embargo, aún existen muchos factores desconocidos en la terapia celular, entre los que se incluyen el mecanismo de acción, los tipos de células que resultan más útiles, las estrategias de administración más eficaces, así como su seguridad. La obtención de imágenes con métodos no invasivos permite utilizar una gran variedad de herramientas para valorar cuantitativamente muchos de estos factores desconocidos. En este artículo nos centramos en la ecocardiografía, la resonancia magnética, la tomografía computarizada, la tomografía por emisión de positrones y la tomografía por emisión de fotón único en el contexto de la terapia celular, para explicar la forma en que estas modalidades de imagen se están utilizando para dar respuesta a muchas de esas cuestiones.

Palabras clave: *Células madre. Imagen por resonancia magnética. Ecocardiografía. Imágenes con radionúclidos.*

Section sponsored by Laboratorio Dr Esteve

INTRODUCTION

Cellular therapeutics have shown early promise for the treatment of cardiovascular diseases. In fact, there are numerous clinical trials underway with goals of achieving myocardial regeneration, revascularization, resynchronization, functional recovery, and reducing remodeling. Promising results from some early clinical trials¹⁻⁴ suggest that pro-

genitor cells and autologous bone marrow-derived stem cells delivered via intracoronary injection can improve myocardial function and have provided impetus for further exploration of cellular therapeutics to treat heart disease. Perhaps the most important basic science question is “What are the mechanisms by which cell therapies act to improve cardiovascular performance?” Proposed mechanisms include neovascularization (either directly or by the release of growth factors), activated cytoprotection via the release of paracrine factors, recruitment and activation of resident stem cells, suppression of inflammation, and myodifferentiation.⁵ Just as important as understanding the mechanisms by which cellular therapeutics work is identifying the most efficacious cell types, evaluating the therapeutic safety, understanding the long term benefits of the therapy, finding how best to deliver the therapy, improving cell engraftment and cell survival, and determining the best way to track the fate of the cell therapy in vivo over time.

Disclosure: Wesley Gilson is an employee of Siemens Corporate Research, Inc.

Funding sources: NIH R21 HL0089029 and MD Stem Cell Research Fund 2008-MSCRFII-0399

Correspondence: Wesley Gilson, PhD, Siemens Corporate Research, Inc, 601 N, Caroline Street, JHOC 3260 Baltimore, MD 21287-0802, USA

Noninvasive imaging can play an important role in studies designed to answer many of these questions. Echocardiography, magnetic resonance imaging (MRI), computed tomography (CT), positron emission tomography (PET), and single photon emission computed tomography (SPECT) are already used clinically to assess myocardial anatomy, function, viability, and perfusion. Incorporation of noninvasive imaging into basic research experiments on cell therapy has significant advantages. In principle, it enables *in vivo* interrogation of the therapeutic effects on anatomy and physiology while reducing the number of animals needed for experiments, allowing serial evaluation of the progression of disease and treatment response, and oftentimes providing more accurate quantitative measurements or even measurements not possible by any other means.

The purpose of this article is to review the different noninvasive modalities used for cardiovascular imaging in the context of their application to studying cellular therapeutics. For each modality, a brief description of the technology will be provided followed by examples of how that technology has been used to evaluate cell therapy efficacy and treatment strategy.

ECHOCARDIOGRAPHY

Echocardiography or cardiac ultrasound is widely used in cardiology clinics worldwide to assess heart size and function, valvular function, and pericardial diseases. The general principle behind ultrasound imaging is that a piezoelectric transducer converts electrical signals to acoustic waves oscillating at frequencies from 2 to 30 MHz. These acoustic waves are transmitted into the body and are reflected as they pass through the different tissue layers. The reflected acoustic waves then, in turn, vibrate the transducer that generated them. These vibrations are converted back into electric signal and sent to the scanner for image processing. Information about the echo duration, frequency and signal intensity are used to generate the ultrasound image. It is important to note that the magnitude of the excitation frequency is directly proportional to the penetration depth of the acoustic wave and to the spatial resolution of the image. Doppler ultrasound is able to measure flow and relative velocity. Contrast-enhanced ultrasound using gas-filled microbubbles can be used to enhance blood-myocardial interfaces, improve the measurement of tissue perfusion and blood flow⁶ and recent developments have been made toward conjugating microbubbles with targeted ligands that bind receptors and would enable targeted delivery of the contrast agents to sites of disease.⁷

Echocardiography has primarily been used to investigate functional changes following cell transplantation. Jin et al⁸ used cardiac ultrasound to show that left ventricular ejection fraction increased significantly in post-infarct rats who received mesenchymal stem cells (MSCs) transplanted within a biodegradable scaffold. Wolf et al⁹ used standard B-mode ultrasound and contrast echocardiography to evaluate intravenous treatment with autologous and allogeneic MSCs in infarcted swine. In this study, myocardial contrast echocardiography showed smaller infarct sizes and improved microvascular flow in ischemic border zones in treated animals; conventional echocardiography demonstrated higher fractional area shortening and improved cardiac synchrony.

Researchers have also begun exploring techniques for delivering and tracking the cells using ultrasound. Bara et al¹⁰ labeled human CD133+ cells with CliniMACS nanoparticles and successfully used transesophageal echocardiography to track the delivery and fate of the cells in a porcine model of myocardial infarction (Figure 1). Others have successfully used ultrasound-mediated microbubbles to target transplantation of MSCs and endothelial progenitor cells to infarcted myocardium.^{12,13}

MAGNETIC RESONANCE IMAGING

MRI is a multi-purpose imaging modality whose versatility is particularly apparent in cardiovascular imaging. It is frequently used to assess cardiac anatomy, ventricular function, myocardial mass, myocardial viability, blood flow, perfusion, and even myocardial energetics. Simplistically, MRI is performed using a strong homogeneous magnetic field to align the nuclear magnetization of the hydrogen atoms or protons of water in the body. Radiofrequency pulses are used to excite the magnetization which leads to signal generation. A group of orthogonal gradient coils is used to alter the magnetic field in a systematic way to achieve spatial encoding of the magnetization, which can be used for image generation. By modifying the timing and order of the sequence of activations of the radiofrequency and gradient pulses, in combination with the natural abundance and relaxation properties (T1 and T2) of the nuclear spins of different tissue types, numerous types of MR images with different contrasts can be generated.

The workhorse of cardiac MRI is the standard cine MRI, which is used primarily to evaluate cardiac anatomy and global function. Regional analysis of parameters, such as wall thickening, can be evaluated by employing approaches such as the AHA 17-segment model.¹⁴ Many studies have used cine MRI to evaluate changes in post-infarction

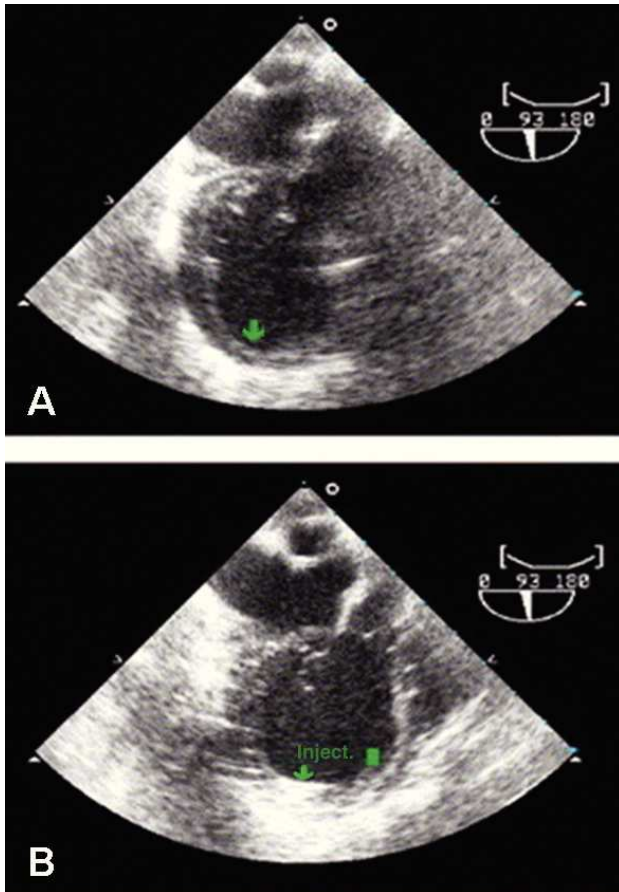


Figure 1. Echocardiographic images of the posterolateral apex before (A) and after (B) engraftment of CliniMACS magnetically labeled CD133-grafted cells. The magnetically labeled cells appeared hyperechoic (green arrows) in post-delivery imaging. Adapted with permission from Ruhparwar et al.¹¹

myocardial function and remodeling following the delivery of cellular therapy.¹⁵⁻²⁰ As an example, Grauss et al¹⁸ recently showed that left ventricular (LV) function was improved and remodeling was reduced in post-infarct mice receiving human MSCs forced to express the cardiomyogenic transcription factor myocardin. Hashemi et al¹⁹ used cine MRI in a placebo-controlled, dose ranging study to evaluate the safety of endomyocardial delivery of allogeneic MSCs post-infarction in pigs.

To tease out the more subtle regional changes in contractile function, including differentiating sub-endocardial from transmural changes, techniques such as myocardial tagging,^{21,22} displacement-encoding imaging,^{23,24} and harmonic phase imaging²⁵ have been applied to animal models of cardiovascular disease. More details about these techniques can be found in a review article by Epstein.²⁶ With the increased resolution of contractile function measurement, studies, such as that by Amado et al,²⁷ have been able to identify a time-dependent recovery of

local contractility associated with the appearance of new tissue resulting from transplantation of allogeneic MSCs in a pig model of myocardial infarction.

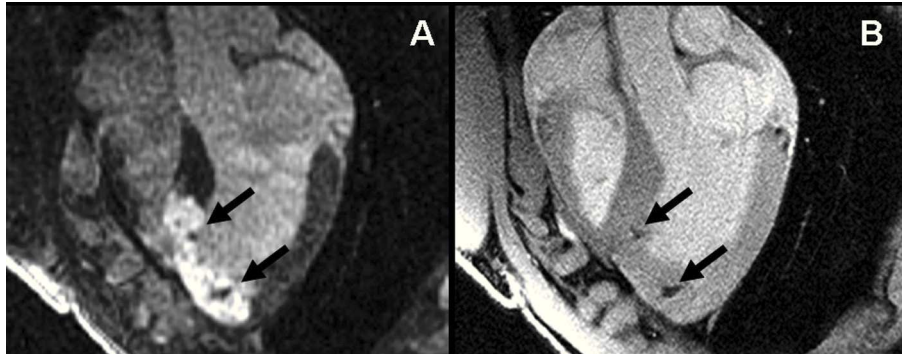
Delayed contrast-enhanced (DCE) MRI has been validated against histological staining as an accurate noninvasive method of infarct sizing.^{28,29} As such, many basic research studies of myocardial infarction have used DCE-MRI to compare infarct size between groups, as well as over the time course of a study.¹⁵ DCE-MRI involves intravenous administration of a paramagnetic contrast agent (eg, Gd-DTPA), waiting approximately 10-15 minutes for the contrast agent to “wash-in” to the infarcted tissue and “wash-out” of the normal myocardium, and imaging using a MRI sequence designed to null the signal in normal myocardium and enhance infarcted myocardium where the contrast agent temporarily collects. An example DCE-MRI image is shown in Figure 2A demonstrating clear delineation of infarcted myocardium.³⁰

Dynamic MR first pass imaging can be applied as an adjunct to DCE-MRI as a means of measuring myocardial perfusion. Using dedicated perfusion-sensitive, heavily T1-weighted MR imaging sequences during the initial infusion of the gadolinium-based contrast agents, myocardial perfusion can be qualitatively and even quantitatively assessed.³¹ A recent study by Schuleri et al³² demonstrated using first-pass perfusion MRI in post-infarct pigs treated with intramyocardial injections of allogeneic MSCs that there is an early increase in myocardial perfusion that precedes subsequent improvements in contractile function and a reduction in apoptosis. Such results could provide important information about the mechanism by which the cell therapy acts to treat the disease.

Though not generally considered an imaging technique, an analogue to MRI is MR spectroscopy. MR spectroscopy offers the ability to investigate myocardial energetics and is available using the same imaging equipment. Zeng et al³³ found using P³¹ MR spectroscopy that one can significantly improve bioenergetics in post-infarct swine, as measured by the subendocardial phosphocreatine/adenosine triphosphate ratio, by transplanting bone marrow-derived multi-potent progenitor cells to borderzone myocardium. Moreover, they were able to demonstrate that these improvements in bioenergetics were supported by improvements in regional and global contractility as measured by cine MRI. Similar results using autologous MSC transplantation have been reported.³⁴

Assessing the anatomic and physiologic response to cellular therapeutics is important, but it is just as important to confirm engraftment and track the fate of the cells. Iron oxide nanoparticles have been used extensively to label and track cells with MRI

Figure 2. Representative long-axis DCE-MRI (A) and T2*-weighted gradient echo MRI (B) of magnetically labeled mesenchymal stem cells within 24 hours of intramyocardial injection. Two injection sites of the iron oxide labeled cells are visualized as hypointense lesions (arrows) in the high resolution gradient echo MRI. These injection sites are also apparent in the DCE-MRI and clearly localized to the hyperintense infarcted myocardium. Adapted from Kraitchman et al.²⁹ DCE indicates delayed contrast-enhanced; MRI, magnetic resonance imaging.



in vivo.^{35,36} Due to their superparamagnetic properties, these particles when internalized by cells make the cells visible as hypointensities in standard MR images. T2*-weighted imaging is the most common MRI method for visualizing these hypointense cell clusters. Accordingly, toxicity studies have confirmed that these iron oxide labels have little to no detrimental effect on cell viability or metabolism.^{35,37} Numerous studies have now been performed using iron oxide nanoparticles to label cells prior to transplantation.^{30,38,39} One early study in post-infarct pigs demonstrated clear visualization of the iron-labeled MSCs immediately post-transplantation and at time points several weeks later (Figure 2B).³⁰ Recently, positive contrast imaging has gained interest as a possible way to improve visualization and sensitivity.⁴⁰⁻⁴²

With clear imaging of the cardiac anatomy and depiction of the infarcted tissue combined with visualization of labeled cellular therapy, MRI provides a wide array of tools for assessing the efficacy and engraftment/fate of the cells. To add to the armamentarium, MR fluoroscopy has been used to achieve real-time guidance of cell therapies to target locations such as infarcted tissue and its borderzone.⁴³⁻⁴⁷ This functionality allows a more accurate and concentrated delivery of the cellular therapeutics to the diseased tissue compared to intravenous or intra-arterial methods and promises to be a more effective means of therapy delivery. However, a lack of commercially-available MR-compatible catheters visible under MRI and able to perform these injections limits the widespread use of these techniques.

COMPUTED TOMOGRAPHY

Cardiac CT is clinically used for coronary artery imaging and to detect aortic aneurysms, aortic dissections, pulmonary embolism, and pericardial disease. Briefly, cardiac CT is an x-ray based imaging modality that provides rapid 3D images of the heart. It is often used with iodine-based con-

trast agents to more clearly visualize the blood vessels. The CT scanner consists of a circular track or gantry with an x-ray tube mounted opposite a detector. During the scan, the tube and detector are rotated around the gantry. As the tube rotates, it emits x-rays which pass through and are absorbed by the subject in the center of the scanner. The remaining x-rays are picked up by the detector. The detected signal is then processed using advanced reconstruction algorithms to generate a 3D CT image. For cardiac CT, an ECG signal can either be used prospectively to gate or trigger image acquisition, or it can be used for retrospective reconstruction.

Similar to MRI, contrast-enhanced multi-detector CT has been validated for viability imaging.⁴⁸ Subsequently, Amado et al²⁷ used cardiac CT in combination with previously described MRI techniques to investigate cardiac regeneration after intramyocardial MSC transplantation in post-infarct swine. Contrast-enhanced CT revealed an increase in sub-endocardial tissue rim thickness and infarct scar reduction over the 8-week study which was supported by a recovery of active contractility in these associated regions as measured by MRI tagging. Furthermore, histology confirmed that this rim contained morphologically normal myocytes.

Microencapsulation techniques in combination with imaging contrast agents^{49,50} have recently been explored as a means of immunoprotecting cells while also providing an environment that allows the free flow of oxygen and nutrients to the cells and cell by-products away from the cells. Using radioopaque contrast agents, Barnett et al⁴⁹ labeled and encapsulated pancreatic islet cells and demonstrated effective glucose responsiveness. Early results using this technique with mesenchymal stem cells⁵¹⁻⁵⁵ have shown promise, particularly in enhancing angiogenesis in a rabbit model of peripheral arterial disease. Example CT images of these x-ray visible microcapsules transplanted in an ex vivo heart are shown in Figure 3.

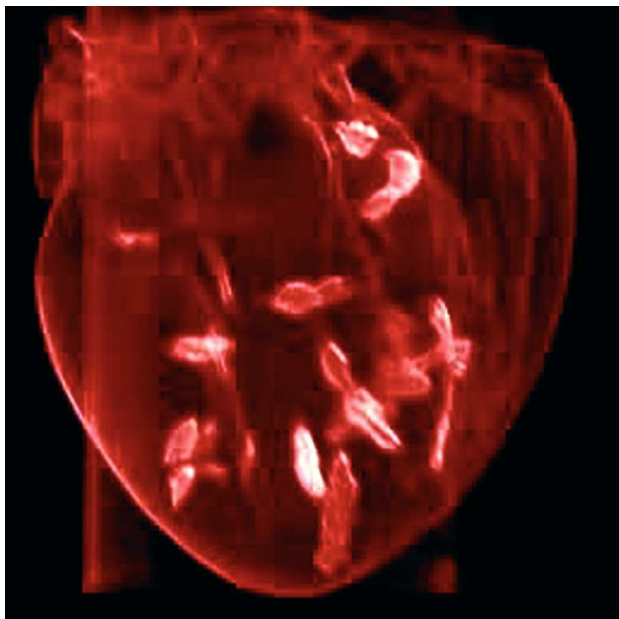


Figure 3. Computed tomography of an excised heart following transplantation of mesenchymal stem cells encapsulated with Barium sulfate. Multiple injections of the microcapsules are clearly visible throughout the heart.

NUCLEAR MEDICINE IMAGING

Nuclear medicine uses radioactive isotopes to interrogate cellular and sub-cellular biological and metabolic processes. Generally, these radioactive isotopes or radionuclides are chemically bound to complexes designed to specifically target certain physiologic processes. These radioactive complexes, often referred to as tracers, are introduced into the body prior to imaging (ie, frequently by intravenous injection). Based on the design of the tracer, the disease process may either be identified by a large uptake of the radioactive tracer or exclusion of the tracer. The 2 most common tomographic nuclear medicine imaging techniques are PET and SPECT.

Positron Emission Tomography

PET imaging operates on the following principle. The PET tracers emit positrons which annihilate with nearby electrons causing 2 gamma photons (511 KeV) to be emitted in opposite directions. The coincident detection of these emissions by multiple detectors in the PET scanner allows direct localization of the annihilation events. Specifically, statistical analysis and tomographic reconstruction are used to generate the 3D PET image. PET radionuclides have short half-lives (ranging from ~20 minutes for ^{11}C , to ~110 minutes for ^{18}F , to ~4.2 days for ^{124}I) and therefore often require that the cyclotron that produces them be on-site or nearby. Ad-

ditionally, this short half-life requires that tracers reach their target in a fairly expeditious manner.

The most common tracer molecule is fluorodeoxyglucose (FDG), a sugar that is tagged with the ^{18}F isotope and used to investigate glucose metabolism. In clinical cardiology, [^{18}F]-FDG PET is most frequently used to identify “hibernating myocardium” or viable heart tissue with metabolically reduced function. Clinically, this hibernating myocardium is considered salvageable if revascularization is performed in the near future.

Though used extensively for viability imaging, PET is also capable of measuring perfusion, contractile function, substrate metabolism, oxygen consumption, autonomic innervation, and angiogenesis.⁵⁶ Therefore, PET imaging can play a valuable role in the thorough evaluation of therapeutic response of cell therapies.

Perhaps the strongest case for PET imaging in the context of cellular therapeutics is its capacity for cell tracking. Radiolabeling of cells for PET imaging can be performed directly with the radionuclide or by way of a reporter gene. Direct labeling involves incubation of cells with the radiotracer to allow sufficient uptake into the cells. Recently, [^{18}F]-FDG has shown success in labeling and tracking tissue distribution of autologous bone marrow mononuclear cells and progenitor cells following intracoronary transplantation in post-infarct pig hearts.⁵⁷⁻⁵⁹ The success of PET with direct labeling is quite promising but is limited primarily by the short half-life of ^{18}F . To date, there has been limited success direct labeling with other longer half-life PET isotopes. Furthermore, similar to magnetic labeling, detection of stem cells directly labeled with radionuclide labeling will be hindered if rapid cell proliferation occurs.

Recent advances in reporter gene-based cell labeling have extended the capabilities of PET imaging beyond short-term monitoring. Reporter genes encode for substances, such as enzymes or receptors, that will bind with a reporter probe. For labeling, a reporter gene is typically transfected exogenously into the cells. Following transplantation, imaging with a PET-specific radionuclide labeled reporter probe enables detection of the cells. More details on reporter gene cell labeling can be found in Bengel et al.⁶⁰ To-date, there are currently 3 types of reporter genes – enzyme-based, receptor-based, and transporter protein-based. Each approach has different advantages and disadvantages as outlined by Zhang et al.⁶¹ Currently, the most common reporter gene-based cell labeling technique for PET imaging has been enzyme-based using the herpes simplex virus type 1 mutant thymidine kinase (*HSV1-tk*) reporter gene in combination with different ^{18}F radionuclide tracers. For example, Wu et al⁶² have published a

study using *HSV1-sr39tk* as a PET reporter gene to track cell survival following intramyocardial transplantation of embryonic rat cardiomyoblasts. In that study, they demonstrated long-term survival of the cells out to 16 days. In a subsequent study by Cao et al⁶³ a novel triple fusion reporter gene for fluorescence, bioluminescence, and PET imaging was developed and used to study cell survival, proliferation, and migration of embryonic stem cells after delivery to the rat myocardium. PET imaging using 9-[4-¹⁸F-fluoro-3-(hydroxymethyl)butyl]guanine (¹⁸F-FHBG) confirmed survival and proliferation as indicated by an increase in PET signal (and bioluminescence) throughout the 4 week time course of the study. Fusion of ¹⁸F-FHBG (labeled cells) and ¹⁸F-FDG (myocardial viability) images from this study demonstrate cell localization using PET (Figure 4).

Recently, PET reporter genes have been used in a relevant large animal model of reperfused myocardial infarction to track biodistribution after direct myocardial injection using an electrical mechanical mapping system.⁶⁴ These studies were performed on a clinical PET scanner and lend promise to similar studies in patients in the future.

Single Photon Emission Computed Tomography

Unlike PET imaging, SPECT operates by directly detecting gamma radiation from the tracer. During a SPECT scan, the gamma camera is rotated around the subject and projection images are acquired. Filtered back projection and iterative reconstruction are used to create a 3D volume of the 2D projection data. Synchronization of the SPECT acquisition with the electrocardiogram is commonly used when quantifying myocardial perfusion, thickness, contractility, and other measures of ventricular function. SPECT imaging may also be used to assess viability, substrate metabolism, and cell death,⁶⁵ all of which can be important in assessing the efficacy of cell therapy and in understanding the mechanisms by which the cell therapies participate in treating the disease.

Similar to PET imaging, cell labeling for SPECT can be divided into direct labeling and reporter gene-based labeling techniques. Direct labeling involves incubation of the cells with radioisotopes such as ¹¹¹In oxine and has been shown to not affect the proliferative capacity of the cells or to negatively affect the surface or intracellular markers.⁶⁵ In general, SPECT radiotracers offer several advantages over PET tracers, such as longer half-lives, increased labeling efficiency, and enhanced stability.⁶¹ SPECT imaging has been used to monitor and track the distribution of direct radionuclide

labeled cellular therapeutics.⁶⁶ In this study, MSCs were directly labeled with ¹¹¹Indium (half-life of 67 hours) and iron oxide nanoparticles. The cells were delivered intravenously to dogs at 3 days after creation of reperfused myocardial infarctions. SPECT imaging was performed at multiple time points up to 8 days post-injection. Although initial uptake was predominantly in the lungs with significant redistribution to the liver, focal and diffuse uptake to the heart was observed in several of the infarcted animals (Figure 5) while no detection was observed in MR images. This study demonstrates the value of SPECT imaging for tracking the biodistribution and fate of the cells after intravenous delivery, and also shows its higher sensitivity for visualizing labeled cells compared to MRI.

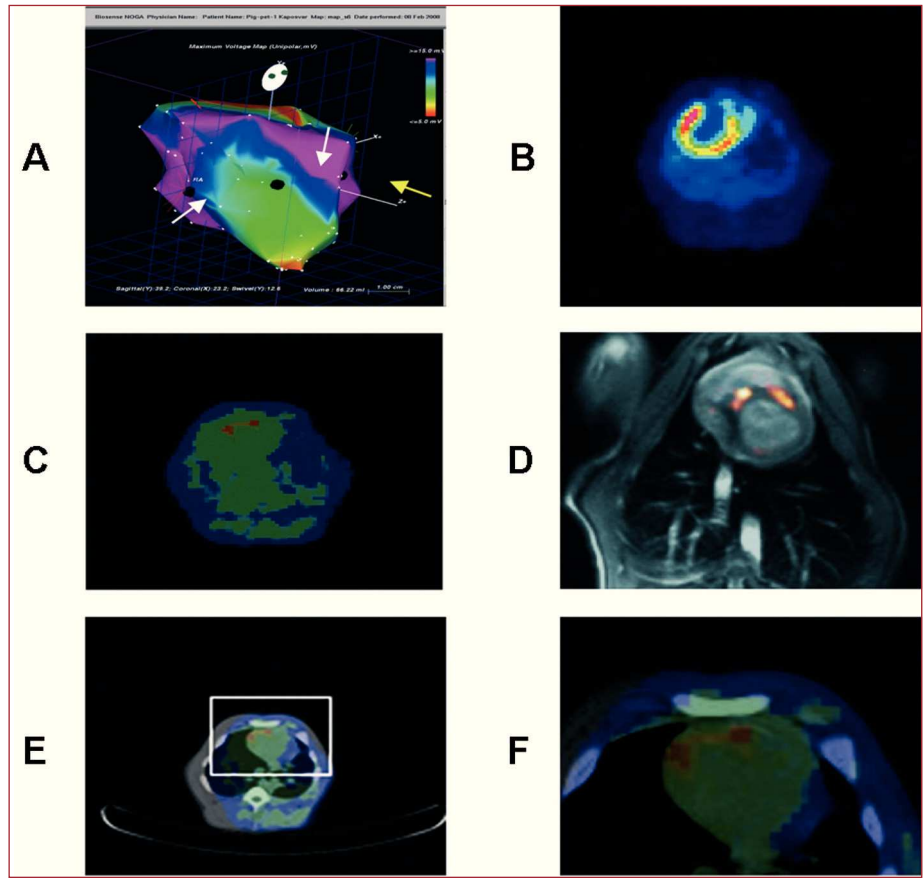
Reporter-gene labeling for SPECT is performed as described for PET imaging by just replacing the substrate label with a single photon emitting radioisotope.^{67,68} For example, Stodilka et al⁶⁹ used ¹¹¹In-labeled MSCs transfected with a reporter gene followed by a systemic injection of ¹³¹I-labeled reporter probe to track the cells in a canine infarcted myocardium. By using a dual-isotope approach, they were able to correct for physical effects such as cross-talk, scatter and attenuation, and subsequently obtain a quantitative evaluation of cell expression. In another study, the sodium-iodide symporter (NIS) was transduced into cardiac-derived stem cells using lentiviral vectors and both ^{99m}Tc (SPECT) and ¹²⁴I (PET) were used to detect and localize the stem cells in vivo.⁷⁰

Because PET and SPECT imaging do not necessarily image anatomy, they are often combined with other imaging techniques, such as CT or MRI, to better localize their results. Recently, the research community and companies have begun integrating these nuclear medicine scanners with the CT and MRI scanners for precise image registration. Furthermore, the anatomical images can be used for attenuation correction to provide more accurate quantification of metabolic activity.

CONCLUSIONS

Noninvasive cardiovascular imaging modalities such as echocardiography, MRI, CT, PET, and SPECT are invaluable for basic science research. By presenting their capabilities in the context of their application to cellular therapeutics, this review has only scratched the surface of their full functionality. However, it should provide a framework by which to begin to understand their importance. Furthermore, it should be stated that numerous other non-invasive modalities exist or are on the horizon⁷¹ that promise to continue to push imaging capabilities for basic science research.

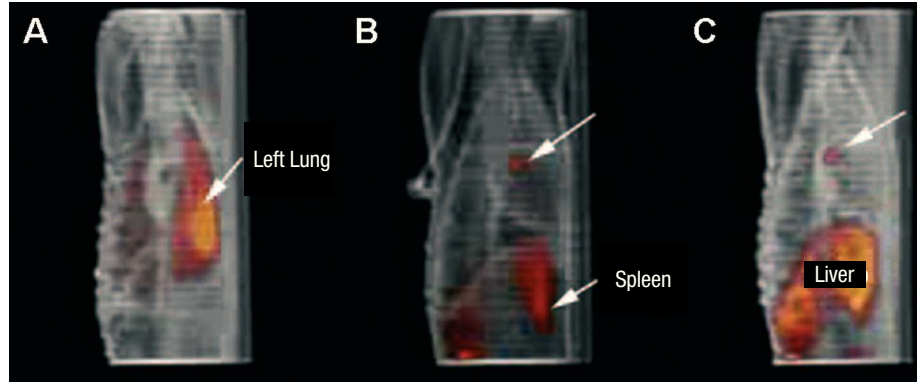
Figure 4. Endocardial mapping of a pig heart 16 days after myocardial infarction. A: a voltage map with the sites (black points) of NOGA (Cordis, Johnson & Johnson)-guided intramyocardial injections of HSV1-tk-transfected MSCs (white arrows at the border zone of infarction) and non-transfected MSCs (yellow arrow at the non-infarcted posterior wall). Normal viability is represented by blue and pink colors. Yellow and green colors represent decreased viability in the mid-distal anterior wall, and red represents non-viability at the heart apex. B: ¹³N ammonia PET with a transmission scan of the pig heart (supine position) 16 days after acute infarction indicating perfusion defect in the anterior wall and apex. C: ¹⁸F-FHBG tracer uptake in the 2 injected points, representing the location of the transfected MSCs 8 h after cell delivery into the myocardium (PET transmission scan, pig in supine position). No activity is seen in the posterior wall, where the non-transfected MSCs were injected. D: a fusion image of MRI (grayscale) and ¹⁸F-FHBG PET (hot scale) indicates tracer accumulation in the sites only where lentiviral vector for transgene expression of the trifusion protein renilla luciferase, red fluorescent protein and herpes simplex truncated thymidine kinase (LV-RL-RFP-tTK-MSC) were intramyocardially injected. E: ¹⁸F-FHBG hybrid PET-CT image for localization of the injected cells in the anterior wall. F: magnification of a region of interest from the ¹⁸F-FHBG-CT. Reprinted with permission from Gyöngysi et al.⁶³ CT indicates computed tomography; MRI, magnetic resonance imaging; ¹⁸F-FHBG, 9-4-¹⁸F-fluoro-3-(hydroxymethyl)butyl]guanine; MSC, mesenchymal stem cells; PET, positron emission tomography.



REFERENCES

1. Wollert KC, Meyer GP, Lotz J, Ringes-Lichtenberg S, Lippolt P, Breidenbach C, et al. Intracoronary autologous bone-marrow cell transfer after myocardial infarction: the BOOST randomised controlled clinical trial. *Lancet*. 2004;364:141-8.
2. Bartunek J, Vanderheyden M, Vandekerckhove B, Mansour S, Bruyne BD, Bondt PD, Haute IV, et al. Intracoronary injection of CD133-positive enriched bone marrow progenitor cells promotes cardiac recovery after recent myocardial infarction: feasibility and safety. *Circulation*. 2005;112 Suppl 9:1178-1183.
3. Schächinger V, Erbs S, Elsässer A, Haberbosch W, Hambrecht R, Hölschermann H, et al. Improved clinical outcome after intracoronary administration of bone-marrow-derived progenitor cells in acute myocardial infarction: final 1-year results of the REPAIR-AMI trial. *Eur Heart J*. 2006;27:2775-83.
4. Dill T, Schächinger V, Rolf A, Möllmann S, Thiele H, Tillmanns H, et al. Intracoronary administration of bone marrow-derived progenitor cells improves left ventricular function in patients at risk for adverse remodeling after acute ST-segment elevation myocardial infarction: results of the reinfusion of enriched progenitor cells and infarct remodeling in acute myocardial infarction study (REPAIR-AMI) cardiac magnetic resonance imaging substudy. *Am Heart J*. 2009;157:541-7.
5. Dimmeler S, Zeiher AM. Cell therapy of acute myocardial infarction: Open questions. *Cardiology*. 2008;113:155-60.
6. Lang RM, Mor-Avi V. Clinical utility of contrast-enhanced echocardiography. *Clin Cardiol*. 2006;29(9 Suppl 1):I15-I25.
7. Villanueva FS. Molecular imaging of cardiovascular disease using ultrasound. *J Nucl Cardiol*. 2008;15:576-86.
8. Jin J, Jeong SI, Shin YM, Lim KS, Soo Shin H, Lee YM, et al. Transplantation of mesenchymal stem cells within a poly(lactide-co-epsilon-caprolactone) scaffold improves cardiac function in a rat myocardial infarction model. *Eur J Heart Fail*. 2009;11:147-53.
9. Wolf D, Reinhard A, Krause U, Seckinger A, Katus HA, Kuecherer H, et al. Stem cell therapy improves myocardial perfusion and cardiac synchronicity: new application for echocardiography. *J Am Soc Echocardiogr*. 2007;20:512-20.
10. Bara C, Ghodsizad A, Niehaus M, Makoui M, Piechaczek C, Martin U, et al. In vivo echocardiographic imaging of transplanted human adult stem cells in the myocardium labeled with clinically applicable CliniMACs nanoparticles. *J Am Soc Echocardiogr*. 2006;19:563-8.
11. Ruhparwar A, Ghodsizad A, Lichtenberg A and Karck M. Visualization of transplanted cells within the myocardium. *Int J Cardiol*. 2008;124:22-26.
12. Zen K, Okigaki M, Hosokawa Y, Adachi Y, Nozawa Y, Takamiya M, et al. Myocardium-targeted delivery

Figure 5. Fused volume renderings of single photon emission tomograms (red) with computed tomograms (gray) of a dog immediately (A), 24 h (B), and 5 days (C) after intravenous administration of Indium-111 oxine-labeled bone marrow-derived mesenchymal stem cells. Initial uptake (A) is predominantly in the lungs and redistributes to the spleen and heart by 24 h (B). At 5 days post-administration, the cells remain visible in the heart with further redistribution to the liver. Reprinted with permission from Kraitchman et al.⁵¹



- of endothelial progenitor cells by ultrasound-mediated microbubble destruction improves cardiac function via an angiogenic response. *J Mol Cell Cardiol.* 2006;40:799-809.
13. Song X, Zhu H, Jin L, Wang J, Yang Q, Jin P, et al. Ultrasound-mediated microbubble destruction enhances the efficacy of bone marrow mesenchymal stem cell transplantation and cardiac function. *Clin Exp Pharmacol Physiol.* 2009;36:267-71.
 14. Cerqueira MD, Weissman NJ, Dilsizian V, Jacobs AK, Kaul S, Laskey WK, et al. Standardized myocardial segmentation and nomenclature for tomographic imaging of the heart: a statement for healthcare professionals from the cardiac imaging committee of the council on clinical cardiology of the American Heart Association. *Circulation.* 2002;105:539-42.
 15. Amado LC, Saliaris AP, Schuleri KH, John MS, Xie JS, Cattaneo S, et al. Cardiac repair with intramyocardial injection of allogeneic mesenchymal stem cells after myocardial infarction. *Proc Natl Acad Sci USA.* 2005;102:11474-9.
 16. Arai T, Kofidis T, Bulte JW, de Bruin J, Venook RD, Berry GJ, et al. Dual in vivo magnetic resonance evaluation of magnetically labeled mouse embryonic stem cells and cardiac function at 1.5 T. *Magn Reson Med.* 2006;55:203-9.
 17. Moelker AD, Baks T, van den Bos EJ, van Geuns RJ, de Feyter PJ, Duncker DJ, et al. Reduction in infarct size, but no functional improvement after bone marrow cell administration in a porcine model of reperfused myocardial infarction. *Eur Heart J.* 2006;27:3057-64.
 18. Grauss RW, van Tuyn J, Steendijk P, Winter EM, Pijnappels DA, Hogers B, et al. Forced myocardin expression enhances the therapeutic effect of human mesenchymal stem cells after transplantation in ischemic mouse hearts. *Stem Cells.* 2008;26:1083-93.
 19. Hashemi SM, Ghods S, Kolodgie FD, Parcham-Azad K, Keane M, Hamamdzi D, et al. A placebo controlled, dose-ranging, safety study of allogeneic mesenchymal stem cells injected by endomyocardial delivery after an acute myocardial infarction. *Eur Heart J.* 2008;29:251-9.
 20. Ziebart T, Yoon CH, Trepels T, Wietelmann A, Braun T, Kiessling F, et al. Sustained persistence of transplanted proangiogenic cells contributes to neovascularization and cardiac function after ischemia. *Circ Res.* 2008;103:1327-34.
 21. Zerhouni EA, Parish DM, Rogers WJ, Yang A, Shapiro EP. Human heart: tagging with MR imaging—a method for noninvasive assessment of myocardial motion. *Radiology.* 1988;169:59-63.
 22. Axel L, Dougherty L. MR imaging of motion with spatial modulation of magnetization. *Radiology.* 1989;171:841-5.
 23. Aletras AH, Ding S, Balaban RS, Wen H. DENSE: displacement encoding with stimulated echoes in cardiac functional MRI. *J Magn Reson.* 1999;137:247-52.
 24. Gilson WD, Yang Z, French BA, Epstein FH. Complementary displacement-encoded MRI for contrast-enhanced infarct detection and quantification of myocardial function in mice. *Magn Reson Med.* 2004;51:744-52.
 25. Garot J, Bluemke DA, Osman NF, Rochitte CE, McVeigh ER, Zerhouni EA, et al. Fast determination of regional myocardial strain fields from tagged cardiac images using harmonic phase MRI. *Circulation.* 2000;101:981-8.
 26. Epstein FH. MR in mouse models of cardiac disease. *NMR Biomed.* 2007;20:238-55.
 27. Amado LC, Schuleri KH, Saliaris AP, Boyle AJ, Helm R, Oskouei B, et al. Multimodality noninvasive imaging demonstrates in vivo cardiac regeneration after mesenchymal stem cell therapy. *J Am Coll Cardiol.* 2006;48:2116-24.
 28. Kim RJ, Fieno DS, Parrish TB, Harris K, Chen EL, Simonetti O, et al. Relationship of MRI delayed contrast enhancement to irreversible injury, infarct age, and contractile function. *Circulation.* 1999;100:1992-2002.
 29. Yang Z, Berr SS, Gilson WD, Toufektsian MC, French BA. Simultaneous evaluation of infarct size and cardiac function in intact mice by contrast-enhanced cardiac magnetic resonance imaging reveals contractile dysfunction in noninfarcted regions early after myocardial infarction. *Circulation.* 2004;109:1161-7.
 30. Kraitchman DL, Heldman AW, Atalar E, Amado LC, Martin BJ, Pittenger MF, et al. In vivo magnetic resonance imaging of mesenchymal stem cells in myocardial infarction. *Circulation.* 2003;107:2290-3.
 31. Gerber BL, Raman SV, Nayak K, Epstein FH, Ferreira P, Axel L, et al. Myocardial first-pass perfusion cardiovascular magnetic resonance: history, theory, and current state of the art. *J Cardiovasc Magn Reson.* 2008;10:18.
 32. Schuleri KH, Amado LC, Boyle AJ, Centola M, Saliaris AP, Gutman MR, et al. Early improvement in cardiac tissue perfusion due to mesenchymal stem cells. *Am J Physiol Heart Circ Physiol.* 2008;294:H2002-11.
 33. Zeng L, Hu Q, Wang X, Mansoor A, Lee J, Feygin J, et al. Bioenergetic and functional consequences of bone marrow-derived multipotent progenitor cell transplantation in hearts

- with postinfarction left ventricular remodeling. *Circulation*. 2007;115:1866-75.
34. Feygin J, Mansoor A, Eckman P, Swingen C, Zhang J. Functional and bioenergetic modulations in the infarct border zone following autologous mesenchymal stem cell transplantation. *Am J Physiol Heart Circ Physiol*. 2007;293:H1772-80.
 35. Bulte JWM, Kraitchman DL. Monitoring cell therapy using iron oxide MR contrast agents. *Curr Pharm Biotechnol*. 2004;5:567-84.
 36. Budde MD, Frank JA. Magnetic tagging of therapeutic cells for MRI. *J Nucl Med*. 2009;50:171-4.
 37. Bulte JWM, Kraitchman DL. Iron oxide MR contrast agents for molecular and cellular imaging. *NMR Biomed*. 2004;17:484-99.
 38. Hill JM, Dick AJ, Raman VK, Thompson RB, Yu ZX, Hinds KA, et al. Serial cardiac magnetic resonance imaging of injected mesenchymal stem cells. *Circulation*. 2003;108:1009-14.
 39. Baklanov DV, Demuinck ED, Thompson CA, Pearlman JD. Novel double contrast MRI technique for intramyocardial detection of percutaneously transplanted autologous cells. *Magn Reson Med*. 2004;52:1438-42.
 40. Stuber M, Gilson WD, Schär M, Kedziorek DA, Hofmann LV, Shah S, et al. Positive contrast visualization of iron oxide-labeled stem cells using inversion-recovery with on-resonant water suppression (IRON). *Magn Reson Med*. 2007;58:1072-7.
 41. Liu W, Dahnke H, Jordan EK, Schaeffter T, Frank JA. In vivo MRI using positive-contrast techniques in detection of cells labeled with superparamagnetic iron oxide nanoparticles. *NMR Biomed*. 2008;21:242-50.
 42. Dahnke H, Liu W, Herzka D, Frank JA, Schaeffter T. Susceptibility gradient mapping (SGM): a new post-processing method for positive contrast generation applied to superparamagnetic iron oxide particle (SPIO)-labeled cells. *Magn Reson Med*. 2008;60:595-603.
 43. Rickers C, Gallegos R, Seethamraju RT, Wang X, Swingen C, Jayaswal A, et al. Applications of magnetic resonance imaging for cardiac stem cell therapy. *J Interv Cardiol*. 2004;17:37-46.
 44. Kraitchman DL, Gilson WD, Lorenz CH. Stem cell therapy: MRI guidance and monitoring. *J Magn Reson Imaging*. 2008;27:299-310.
 45. Lederman RJ, Guttman MA, Peters DC, Thompson RB, Sorger JM, Dick AJ, et al. Catheter-based endomyocardial injection with real-time magnetic resonance imaging. *Circulation*. 2002;105:1282-4.
 46. Dick AJ, Guttman MA, Raman VK, Peters DC, Pessanha BSS, Hill JM, et al. Magnetic resonance fluoroscopy allows targeted delivery of mesenchymal stem cells to infarct borders in swine. *Circulation*. 2003;108:2899-904.
 47. Saeed M, Martin AJ, Lee RJ, Weber O, Revel D, Saloner D, et al. MR guidance of targeted injections into border and core of scarred myocardium in pigs. *Radiology*. 2006;240:419-26.
 48. Lardo AC, Cordeiro MAS, Silva C, Amado LC, George RT, Saliaris AP, et al. Contrast-enhanced multi-detector computed tomography viability imaging after myocardial infarction: characterization of myocyte death, microvascular obstruction, and chronic scar. *Circulation*. 2006;113:394-404.
 49. Barnett BP, Kraitchman DL, Lauzon C, Magee CA, Walczak P, Gilson WD, et al. Radiopaque alginate microcapsules for x-ray visualization and immunoprotection of cellular therapeutics. *Mol Pharm*. 2006;3:531-38.
 50. Barnett BP, Arepally A, Karmarkar PV, Qian D, Gilson WD, Walczak P, et al. Magnetic resonance-guided, real-time targeted delivery and imaging of magnetocapsules immunoprotecting pancreatic islet cells. *Nat Med*. 2007;13:986-91.
 51. Kraitchman DL, Kedziorek DA, Cosby K, Gilson WD, Huang G, Kohl T, et al. X-ray visible stem cell therapy enhances angiogenesis in a rabbit model of peripheral arterial disease. abstract. *J Am Coll Cardiol*. 2008;51:A315.
 52. Kraitchman DL, Bulte JW. In vivo imaging of stem cells and beta cells using direct cell labeling and reporter gene methods. *Arterioscler Thromb Vasc Biol*. 2009 [Epub ahead of print].
 53. Kedziorek DA, Walczak P, Fu Y, Ehtiati T, Brost AB, Azene N, et al. Precise targeting of x-ray-visible microencapsulated mesenchymal stem cells using c-arm CT for interrogation of a bioluminescent reporter gene probe. *J Nucl Med*. 2009;50:657-54. Tsui BMW, Kraitchman DL. Recent advances in small-animal cardiovascular imaging. *J Nucl Med*. 2009;50:667-70.
 55. Nahrendorf M, Sosnovik D, French B, Swirski F, Bengel F, Sadeghi M, et al. Multimodality cardiovascular molecular imaging - part II. *Circ Cardiovasc Imaging*. 2009;2:56-70.
 56. Bengel FM. Nuclear imaging in cardiac cell therapy. *Heart Fail Rev*. 2006;11:325-32.
 57. Doyle B, Kemp BJ, Chareonthaitawee P, Reed C, Schmeckpeper J, Sorajja P, et al. Dynamic tracking during intracoronary injection of 18F-FDG-labeled progenitor cell therapy for acute myocardial infarction. *J Nucl Med*. 2007;48:1708-14.
 58. Hofmann M, Wollert KC, Meyer GP, Menke A, Arseniev L, Hertenstein B, et al. Monitoring of bone marrow cell homing into the infarcted human myocardium. *Circulation*. 2005;111:2198-202.
 59. Qian H, Yang Y, Huang J, Gao R, Dou K, Yang G, et al. Intracoronary delivery of autologous bone marrow mononuclear cells radiolabeled by 18F-fluoro-deoxy-glucose: tissue distribution and impact on post-infarct swine hearts. *J Cell Biochem*. 2007;102:64-74.
 60. Bengel FM, Schachinger V, Dimmeler S. Cell-based therapies and imaging in cardiology. *Eur J Nucl Med Mol Imaging*. 2005;32 Suppl 2:S404-S416.
 61. Zhang Y, Ruel M, Beanlands RSB, deKemp RA, Suuronen EJ, DaSilva JN. Tracking stem cell therapy in the myocardium: applications of positron emission tomography. *Curr Pharm Des*. 2008;14:3835-53.
 62. Wu JC, Chen IY, Sundaesan G, Min JJ, De A, Qiao JH, et al. Molecular imaging of cardiac cell transplantation in living animals using optical bioluminescence and positron emission tomography. *Circulation*. 2003;108:1302-5.
 63. Cao F, Lin S, Xie X, Ray P, Patel M, Zhang X, et al. In vivo visualization of embryonic stem cell survival, proliferation, and migration after cardiac delivery. *Circulation*. 2006;113:1005-14.
 64. Gyöngysi M, Blanco J, Marian T, Trón L, Petneházy, Petrasi Z, et al. Serial non-invasive in vivo positron emission tomographic (PET) tracking of percutaneously intramyocardially injected autologous porcine mesenchymal stem cells modified for transgene reporter gene expression. *Circ Cardiovasc Imaging*. 2009;1:94-103.
 65. Bindeslev L, Haack-Sørensen M, Bisgaard K, Kragh L, Mortensen S, Hesse B, et al. Labelling of human mesenchymal stem cells with indium-111 for SPECT imaging: effect on cell proliferation and differentiation. *Eur J Nucl Med Mol Imaging*. 2006;33:1171-7.
 66. Kraitchman DL, Tatsumi M, Gilson WD, Ishimori T, Kedziorek D, Walczak P, et al. Dynamic imaging of allogeneic

- mesenchymal stem cells trafficking to myocardial infarction. *Circulation*. 2005;112:1451-61.
67. Acton PD, Zhou R. Imaging reporter genes for cell tracking with PET and SPECT. *Q J Nucl Med Mol Imaging*. 2005;49:349-60.
68. Inubushi M, Tamaki N. Radionuclide reporter gene imaging for cardiac gene therapy. *Eur J Nucl Med Mol Imaging*. 2007;34 Suppl 1:S27-S33.
69. Stodilka RZ, Blackwood KJ, Kong H, Prato FS. A method for quantitative cell tracking using SPECT for the evaluation of myocardial stem cell therapy. *Nucl Med Commun*. 2006;27:807-13.
70. Terrovitis J, Kwok KF, Lautamäki R, Engles JM, Barth AS, Kizana E, et al. Ectopic expression of the sodium-iodide symporter enables imaging of transplanted cardiac stem cells in vivo by single-photon emission computed tomography or positron emission tomography. *J Am Coll Cardiol*. 2008;52:1652-60.
71. McVeigh ER. Emerging imaging techniques. *Circ Res*. 2006;98:879-86.